

論文 / 著書情報
Article / Book Information

Title	Tension Control Method Utilizing Antagonistic Tension to Enlarge the Workspace of Coupled Tendon-driven Articulated Manipulator
Authors	Atsushi Takata, Hiroyuki Nabae, Koichi Suzumori, Gen Endo
Citation	IEEE Robotics and Automation Letters, Volume 6, Issue 4, pp. 6647-6653
Pub. date	2021, 9
Copyright	(c) 2021 IEEE. Personal use of this material is permitted. Permission from IEEE must be obtained for all other uses, in any current or future media, including reprinting/republishing this material for advertising or promotional purposes, creating new collective works, for resale or redistribution to servers or lists, or reuse of any copyrighted component of this work in other works.
DOI	https://dx.doi.org/10.1109/LRA.2021.3094489
Note	This file is author (final) version.

Tension Control Method Utilizing Antagonistic Tension to Enlarge the Workspace of Coupled Tendon-driven Articulated Manipulator

Atsushi Takata¹, Hiroyuki Nabae¹, Koichi Suzumori¹, and Gen Endo¹

Abstract—The exploration and inspection of narrow spaces in industrial plants require the use of long-reach redundant manipulators with large three-dimensional (3D) workspaces. To this end, in a previous work, a coupled tendon-driven articulated manipulator with a total length of 10 m and yaw joints for 3D motion was developed. This study focuses on employing the antagonistic tension in a yaw joint to support a tendon that drives a pitch joint with high gravitational loading. Herein, a tension control method that employs the antagonistic tension to reduce the amount of tension required to support the weight of an arm is proposed. The effectiveness of the proposed method is evaluated based on the workspace volume of the previously developed Super Dragon, and the results demonstrate that the proposed method expands the workspace by up to 45%.

Index Terms—Tendon/wire mechanism, redundant robots, serial manipulator

I. INTRODUCTION

TO enable the exploration of narrow spaces in industrial plants, particularly nuclear facilities, long-reach redundant manipulators with large workspaces are being studied actively. However, the use of a long body introduces the problem of enhanced gravitational torques. In our previous work, we developed Super Dragon, a 10-m-long tendon-driven articulated manipulator, which is presented in Fig. 1 [1]. Its redundantly coupled tendons support a large torque on the proximal pitch joint.

This paper addresses the actuation redundancy resolution problem to develop an approach for supporting the weight of a manipulator with as little tension as possible. To motivate this problem, redundant serial mechanisms with more than six degrees of freedom (DOFs) were analyzed. The redundant serial mechanisms were categorized into two groups.

The first group comprises continuum robots that apply no specific mechanical method to support their arms against gravity. OctArm is a continuum robot actuated by artificial



Fig. 1. Super Dragon: a 10-m-long coupled tendon-driven articulated manipulator [1].

muscles. It achieves dexterous manipulation in both air and water [2]. However, its ability to scale-up is limited by the force/weight ratio of the actuator. Although slim and lightweight tendon-driven continuum arms have been developed [3] and studied in the contexts of surgery [4], [5] and industrial plant inspection [6], the structure of a tendon-driven continuum robot comprising multiple joint segments, tendons, and a flexible backbone will have difficulties in enduring large compressive forces owing to its complicated mechanism. As a result, the maximum lengths of previously developed continuum robots were limited to 2–3 m, and it is unlikely that a continuum robot will soon be scaled up to a length that can be applied for plant inspections.

The second category comprises articulated mechanisms that use specific mechanical methods to support themselves against gravity. Owing to the use of these gravity support mechanisms, such articulated mechanisms can feature significantly longer structures. For example, Veolia Nuclear Solutions and Mitsubishi Heavy Industry are developing a planar manipulator with a length of 22 m and a mass of 4600 kg for insertion into the primary containment vessel of the Fukushima Daiichi nuclear power plant [7]. Because the basic movement of the arm occurs on the horizontal plane, its own weight is not loaded onto the actuators. However, this reduces the workspace along the vertical direction. Another example is the PAC robot [8], which is a manipulator for use in nuclear energy facilities and has a total length of approximately 6 m. The robot has a weight compensation mechanism involving a spring and a

Manuscript received: February, 24, 2021; Revised May, 19, 2021; Accepted June, 18, 2021.

This paper was recommended for publication by Editor Clement Gosselin upon evaluation of the Associate Editor and Reviewers' comments. *This study is based on the results obtained from a project commissioned by the New Energy and Industrial Technology Development Organization (NEDO). This work was financially supported by JAEA Nuclear Energy S&T and Human Resource Development Project through concentrating wisdom Grant Number JPJA19P 19210348.

¹Atsushi Takata, Hiroyuki Nabae, Koichi Suzumori, and Gen Endo are with the Department of Mechanical Engineering, Tokyo Institute of Technology, 2-12-1 Ookayama, Meguro-ku, Tokyo 152-8550, Japan takata.a.ac@m.titech.ac.jp

Digital Object Identifier (DOI): see top of this page.

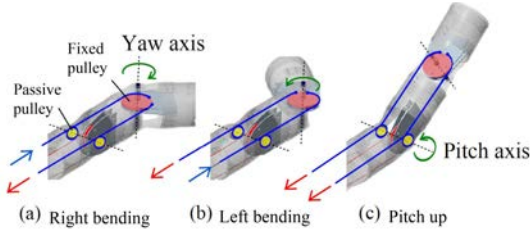


Fig. 2. Antagonistic tension on a yaw joint generates torque on a proximal joint [10].

four-bar linkage to aid the actuators in generating vertical movements. However, this limits the range of the joints in the vertical direction.

In our previous work, we used a coupled tendon-driven mechanism [9] comprising a series of pulleys and tendons, in order to achieve a wider range for the joints, as compared to that in other mechanical designs. At first, this mechanism was proposed as a vertical planar arm with only pitch joints. A design method to install yaw joints, as shown in Fig. 2, was also introduced [10]. The introduction of yaw joints facilitates a 3D workspace.

A workspace of the arm is limited by the tension strength, albeit the strongest tendons available are used. In other words, the tension control method adopted is important, because the tension that supports the high gravity joint torque must be determined to ensure that it does not exceed the design load. Moreover, the actuation redundancy further complicates these methods.

In this study, we focus on the antagonistic tension caused by actuation redundancy. Antagonistic tension is the smaller of the tensions in a pair of tendons pulling one joint. The torque on a joint is generated by the difference between this pair of tensions and not by antagonistic tension. However, the antagonistic tension of a yaw joint generates torque on the proximal pitch joints, as shown in Fig. 2. On the other hand, the antagonistic tension on a pitch joint does not serve to support the other joints.

Redundancy resolution and tension control methods for tendon-driven manipulators have been studied previously. The most commonly used, conventional resolution approach is the pseudo-inverse matrix method [9], [11], [12]. Iterative algorithms for solving linear problems [13], [14], non-iterative polynomial formulations [15], a closed-form solution using the infinity norm [16], and a sequential calculation method for specific mechanism [17] have also been proposed.

However, previous studies made no distinction between the controlling strategies for joints with large gravitational loads and those for the more lightly loaded joints. We presume that this is because these studies primarily investigated planar robot arms or short arms under light gravitational loads, where gravitational torque is not a significant problem. For long tendon-driven articulated arms, however, a high tension is required in the tendons that drive the pitch joint. In these cases, it is preferable to avoid further increasing the antagonistic tension of the pitch joint. However, it is possible to utilize the antagonistic tension of the yaw joint to enlarge the workspace.

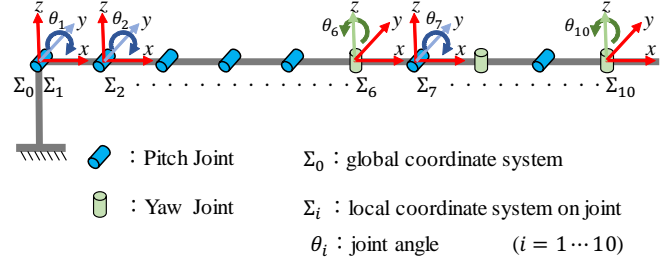


Fig. 3. Kinematically redundant joint configuration of Super Dragon.

In this paper, we propose a tension control method that utilizes the antagonistic tension on the yaw joints to support the arm's weight with less tension than that in the previous methods. The effectiveness of the proposed method is evaluated via a computation of the workspace of the Super Dragon developed in our previous study. Finally, we describe the results of the experiments to determine whether Super Dragon could reach the target positions located in the expanded parts of its workspace.

The remainder of this paper is organized as follows. Section II describes the coupled tendon-driven articulated manipulator. Section III describes previous tension control methods and the proposed method. Section IV describes the computation of the Super Dragon's workspace via the Monte Carlo method and a comparison of workspaces obtained using the tension control methods. Section V describes the results of an experiment using the actual manipulator, and Section VI concludes the paper.

II. COUPLED TENDON-DRIVEN MANIPULATOR

Super Dragon is a coupled tendon-driven articulated manipulator with 10 joints and a total length of 10 m [1]. The joint configuration and coordinate system are shown in Fig. 3. Super Dragon has three yaw joints, i.e., joints 6, 8, and 10, as shown in Fig. 3. All the joints have a range of motion within $\pm 90^\circ$. Figure 4 shows the arrangement of the tendons and pulleys. The joints are driven by 21 tendons. All the actuators that pull the tendons are located at the base of the manipulator. One end of each tendon is fixed to a joint that is driven by it. The other end is guided to the base while being wound around the passive pulleys at the joints closer to the base than to the driven joint, and it is fixed to an actuator on the base. The blue and red lines in the figure represent the joint control tendons (JCTs), which are actuated via electromagnetic motors and control the joint angles. The design load of each JCT is 3 kN. The green line represents the weight compensation tendon (WCT), which is pulled by a pneumatic cylinder with a maximum force of 30.2 kN. The combination of one thick tendon and a set of double pulleys can support most gravitational torques on the five proximal joints. The principle of this mechanism has been explained in [14].

The statics of the manipulator have been explained in [9]. By applying the principle of virtual work to the actuators and joint angles, the relationship between the joint torque $\tau \in$

$\mathbb{R}^{10 \times 1}$ and tension of the tendons $\mathbf{f} \in \mathbb{R}^{21 \times 1}$ can be expressed using Eq. (1), as follows:

$$\boldsymbol{\tau} = \mathbf{R}\mathbf{f} \quad (1)$$

where the radii of the pulleys are $\mathbf{R} \in \mathbb{R}^{10 \times 21}$, the tension in the JCTs is $\mathbf{f}_j \in \mathbb{R}^{20 \times 1}$, the tension in the WCT is f_{wc} , and the tension vector is written as $\mathbf{f} = [\mathbf{f}_j^\top f_{wc}^\top]^\top$. The pulley radius, \mathbf{R} , is also called the structure matrix. In the case of Super Dragon, \mathbf{R} is an upper pseudo-triangular matrix (as described in the Appendix of our previous work [1]). This formulation explains how the load on one tendon is reduced by supporting the proximal joints with several tendons. However, despite the contribution of this mechanism, the tendon must still support a large tension. Ultra-high polyethylene (UHPE) ropes with diameters of 2 mm (DB-96HSL, Hayami industry, strength 4.2 kN) are used as JCTs. A UHPE rope is stronger than a stainless-steel wire rope of the same diameter (e.g., SC-200, SHINYO, strength 3.6 kN) and also possesses the flexibility required for fixing a terminal without undergoing a reduction in its strength [18]. The tension control method and the high-strength tendons function together to enable the operation of a long-reach manipulator. A PBO rope (ZB-15728, Hayami industry) with a diameter of 5.5 mm is used as the WCT. This rope has a sufficiently high strength.

III. REDUNDANCY RESOLUTION FOR TENSION CONTROL

A. Previous Tension Control Methods

In Eq. (1), determining the tension \mathbf{f} from the joint torques $\boldsymbol{\tau}$ is a redundant problem. Moreover, all the tendons must exceed a positive minimum tension \mathbf{f}_{\min} , as shown in Eq. (2). The most prominent conventional method for solving this problem is to use the pseudo-inverse matrix of the structure matrix. The unified tendon-traction control (UTC) method proposed by Ma [9] is suitable for this purpose and has been also used in other studies [11]. The UTC solution is expressed as Eq. (3), in which \mathbf{R}^+ is the pseudo-inverse matrix of \mathbf{R} and \mathbf{E} is the identity matrix. The second term on the right-hand side of Eq. (3) represents the null space, which corresponds to the actuation redundancy. The vector \mathbf{f}_0 , which has positive values and a termed bias tension, is necessary to satisfy Eq. (2). Thus, UTC utilizes redundancy to maintain a positive tension. A flowchart of UTC is presented in the red block of Fig. 5. The advantage of the pseudo-inverse method is that it can be widely used and can be applied via various methods depending on the approach used to address the null space. For example, actuation redundancy is also important in the control of parallel tendon-driven robots, and it is widely applied in these by using an equation very similar to Eq. (1). A method to adjust solutions by changing indices [19] and a global optimization method [20] have also been studied. The disadvantage of the pseudo-inverse methods is that it is difficult for them to consider some features of particular mechanisms, such as a yaw antagonistic tension, upon which this study focuses.

$$\mathbf{f} \geq \mathbf{f}_{\min} \geq \mathbf{0} \quad (2)$$

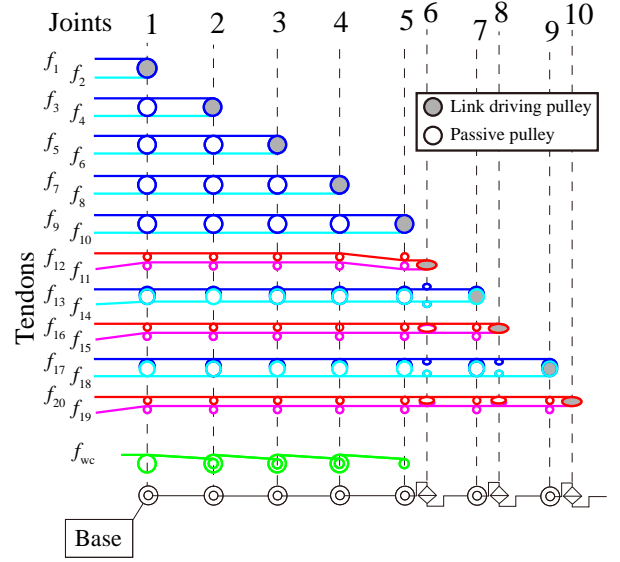


Fig. 4. Arrangement of tendons. The red, green, and blue lines represent 21 tendons actuating 10 joints. On each joint, there are two types of pulleys. Solid circles represent the pulleys driving links. Open circles represent the passively rotatable pulleys.

$$\mathbf{f} = \mathbf{R}^+ \boldsymbol{\tau} + (\mathbf{E} - \mathbf{R}^+ \mathbf{R}) \mathbf{f}_0 \quad (3)$$

Another approach is to use the torque resolver (TR) proposed by Lee and Tasi [17]. The TR is applicable only when the structure matrix is a pseudo-triangular matrix. However, it offers the advantage of a reduced computational time. In this method, actuation redundancy is solved by determining the tension in order from the most distal to the most proximal joint (i.e., $i = n \cdots 1$). In the case of Super Dragon, the tension \mathbf{f}_j is obtained by using Eqs. (4) and (5), and the required torque τ_i^{req} is generated by the tensions \mathbf{f}_{2i-1} and \mathbf{f}_{2i} . It is clear that \mathbf{f}_a is an antagonistic tension that corresponds to the actuation redundancy. $r_{i,j}$ represents the element in the i -th row and j -th column of \mathbf{R} . In this paper, the TR process is expressed as in Eq. (6), in which \mathbf{f}_j is the output of the TR with the required torque $\boldsymbol{\tau}$, antagonistic tension $\mathbf{f}_a \in \mathbb{R}^{10 \times 1}$, and \mathbf{f}_w .

$$\tau_i^{\text{req}} = \tau_i - \sum_{k=i+1}^n (r_{i,2k-1} f_{2k-1} - r_{i,2j} f_{2k}) - r_{i,21} f_w \quad (4)$$

$$\begin{cases} \text{for } \tau_i^{\text{req}} < 0 \\ \text{for } \tau_i^{\text{req}} \geq 0 \end{cases} \begin{cases} f_{2i-1} = \tau_i^{\text{req}} / r_{i,2i-1} + f_a \ i \\ f_{2i} = f_a \ i \\ f_{2i-1} = f_a \ i \\ f_{2i} = \tau_i^{\text{req}} / r_{i,2i} + f_a \ i \end{cases} \quad (5)$$

$$\mathbf{f}_j = \text{TR}(\boldsymbol{\tau}, \mathbf{f}_a, \mathbf{f}_w) \quad (6)$$

Super Dragon is fairly unique in that it features a WCT, making it necessary to determine the WCT tension f_w apart from acquiring the tensions of the JCTs \mathbf{f}_j by using TR. In our previous study [14], f_w of the WCT tension was determined using gradient descent, as shown in Eqs. (7) and (8). The

maximum JCTs tension was used as the objective function. In Eq. (8), n is the number of iterations and α is a small constant. A flowchart showing the application of this method to Super Dragon is presented in the yellow block in Fig. 5 .

$$\mathbf{F} = [f_w] \quad (7)$$

$$\mathbf{F}_{n+1} = \mathbf{F}_n - \alpha \frac{\partial (\max(\mathbf{f}_j))}{\partial \mathbf{F}} \quad (8)$$

In many previous studies, antagonistic tension was primarily applied to prevent tendon sagging or to achieve variable joint stiffness [12]. However, in a coupled tendondriven articulated manipulator, the antagonistic tension of the yaw joint can assist the proximal pitch joint. Thereby a new tension control method is feasible. To the best of our knowledge, no previous study has explored the use of antagonistic tension to support the gravitational joint torque with as little tendon tension as possible.

B. Proposed Method Utilizing Antagonistic Tension

This section describes the combination of the TR approach with optimization calculations for the development of a tension control method called antagonistic tension gradient descent (ATGD). This method updates the antagonistic tension in the yaw joint toward a solution that effectively supports the other tendons.

The optimized parameter contains the antagonistic tensions of three yaw joints. It should be noted that the antagonistic tensions in the pitch joints remain constant. In the case of Super Dragon, as mentioned above, the tension in the WCT, f_w , is also added to the parameters according to Eq. (9). Furthermore, the maximum tensions in the JCTs are used in an objective function for minimization. This is because the objective of the proposed method is to support the weight of an arm with reduced tension. WCT tension is not included in the objective function because it possesses sufficient strength. The parameters \mathbf{F} are updated using a gradient descent method, as shown in Eq. (8). A flowchart of this process is presented in the blue block in Fig. 5 .

$$\mathbf{F} = [f_{a6} \quad f_{a8} \quad f_{a10} \quad f_w] \quad (9)$$

IV. WORKSPACE COMPUTATION

A. Definition of Workspace

The proposed ATGD method was evaluated based on the workspace that could be achieved by Super Dragon. Considering the application of inspecting a plant by using a camera, the workspace was defined as the set of tip positions (three DOFs) that could be reached by employing a tension lower than the design load. Although the Monte Carlo method is often used to calculate this type of workspace [21], [22], it should be noted that, as a result of kinematic redundancy, there are numerous joint angle solutions that achieve a particular tip position. In other words, as the joint angles alter the gravitational torque, the workspace in which a tendon can support the gravitational torque depends on how to solve the redundant inverse kinematics.

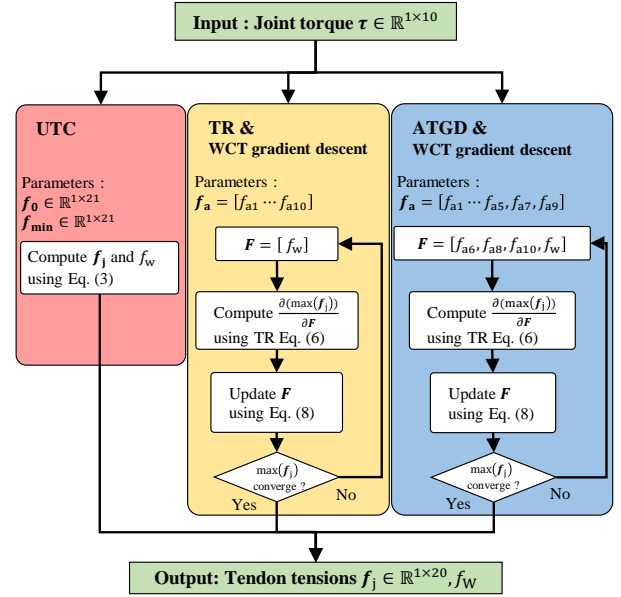


Fig. 5. Flowcharts of the UTC, TR, and ATGD for Super Dragon.

The inverse kinematics of redundant manipulators were actively studied in the 1980 s. In a pioneering study, Nakamura solved the kinematic redundancy of an articulated robot arm using the null space of the Jacobian matrix and applied this approach to manipulation and subtask operations by simultaneously using an arbitrary objective function $\psi(\theta)$ [23]. In the case of Super Dragon, the position of the tip of the manipulator is $x \in \mathbb{R}^{3 \times 1}$, the joint angles are $\theta \in \mathbb{R}^{10 \times 1}$, and the Jacobian matrix is $\mathbf{J} \in \mathbb{R}^{3 \times 10}$. The redundant inverse kinematics are solved via Newton's method using Eq. (10):

$$\delta \theta = \mathbf{J}^+ \delta x + (\mathbf{E} - \mathbf{J}^+ \mathbf{J}) \kappa \frac{\partial \psi}{\partial \theta} \quad (10)$$

where \mathbf{J}^+ is the pseudo-inverse of the Jacobian matrix and κ is a small constant. This methodology has been used for obstacle avoidance [24] and joint torque minimization [25], which are frequently selected as subtasks. In a previous study on the inverse kinematics of a coupled tendon-driven manipulator, Ma solved the inverse kinematics with actuation and kinematic redundancies by minimizing the squared norm of the tendon tension as an objective function [26], with the goals of reducing energy consumption and minimizing joint torque.

In our study, we chose the maximum tension of the JCTs—specifically, $\psi = \max(\mathbf{f}_j)$ —as the objective function. The calculation proceeds so as to increase the maximum tension. If the maximum tension of the inverse kinematics results obtained through this objective function does not exceed the design load, all the kinematics solutions support the weight of the manipulator with a maximum tension below the design load. In other words, a workspace that assumes the worst-case scenario for a tendon is obtained. By considering the need for kinematic redundancy in avoiding obstacles when performing inspection tasks, the workspace obtained using this method is suitable for the evaluation of the tension control method.

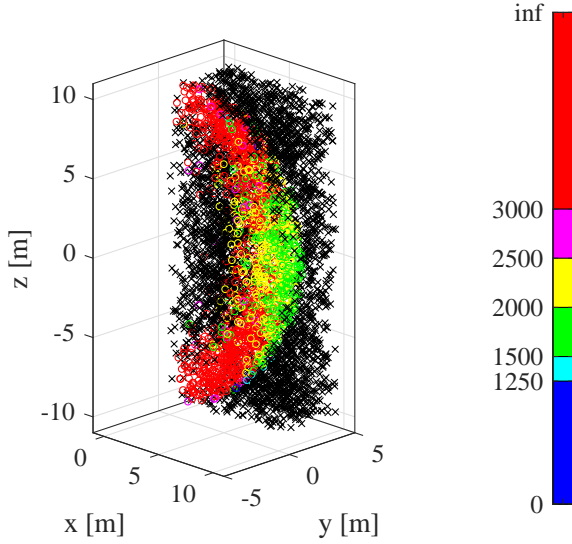


Fig. 6. The computational result obtained via UTC. The cross marks represent the points that are kinematically unreachable.

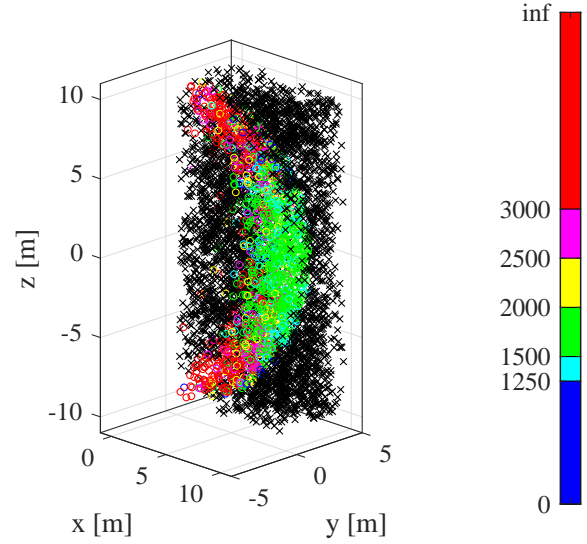


Fig. 8. The computational result obtained via ATGD.

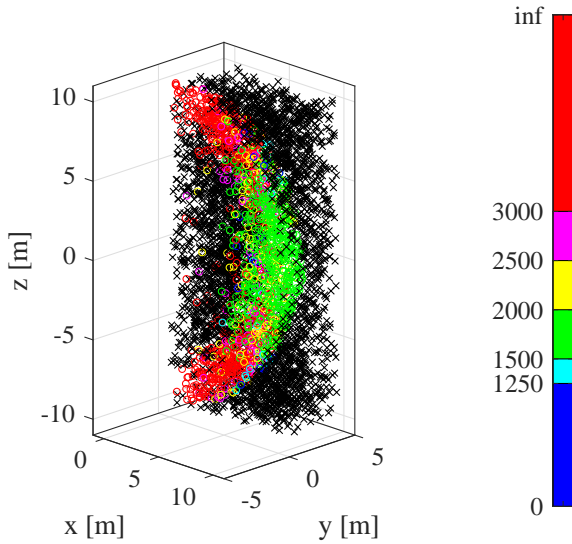


Fig. 7. The computational result obtained via TR.

B. Calculation Conditions

To compute a workspace, a total of 5,000 tip positions were randomly generated in the range of $x = [0 \ 10]$, $y = [0 \ 4.5]$, $z = [-10 \ 10]$, which is sufficiently large when compared to the length of the Super Dragon. It was assumed that the workspace was symmetric with respect to the $x - z$ plane.

The joint angles θ and the tension of the tendons f were calculated for each tip position by using Eq. (10) and $\psi = \max(f_j)$. The tension f was calculated using one of the tension control methods, and the gravitational torques τ were computed from the lengths and weights of the links.

As tension control methods, the UTC, TR, and ATGD

approaches, as shown in Fig. 5, were employed. For the application of UTC, the lower limit of the tension, f_{\min} , and the bias tension, f_0 , shown in Eqs. (2) and (3) were set as follows:

$$f_{\min} = [30 \ 30 \ \dots \ 30 \ 1000]^T [\text{N}] \quad (11)$$

$$f_0 = [30 \ 30 \ \dots \ 30 \ 13000]^T [\text{N}] \quad (12)$$

For the application of TR and ATGD, all antagonistic tensions f_a were set to 100 N. The upper limit of the WCT tension, f_w , was set to 15 kN. All the calculations were implemented in MATLAB. For the UTC and ATGD processes, an Intel Core i7-8700 3.2 GHz with 12 GB RAM was used. For the TR process, an Intel Core i9-9900 3.6 GHz with 16 GB RAM was used.

C. Computational Results

Figure 6 shows the computational results obtained using UTC, Fig. 7 illustrates the results obtained using TR, and Fig. 8 illustrates the results obtained via the proposed method, ATGD. The cross marks represent the points at which no inverse kinematic solution exists. The colors of the open circles indicate the maximum tension values, $\max(f_j)$. The values in red are larger tension, whereas those in blue are smaller tension. Figure 9 shows the polygons of the workspaces at a design load of 3 kN. The red, blue, and yellow polygons represent the workspaces obtained via UTC, ATGD, and TR, respectively. The UTC workspace was obtained by extracting the points below the design load from the results shown in Fig. 6. Similarly, the TR and ATGD workspaces were obtained from Figs. 7 and 8, respectively. The upper right subfigure of Fig. 9 shows a trimetric view. All the other subfigures show trihedral views. Each computation was performed once over computational times of approximately 134, 22.3, and 11.5 h for the ATGD, UTC, and TR cases, respectively.

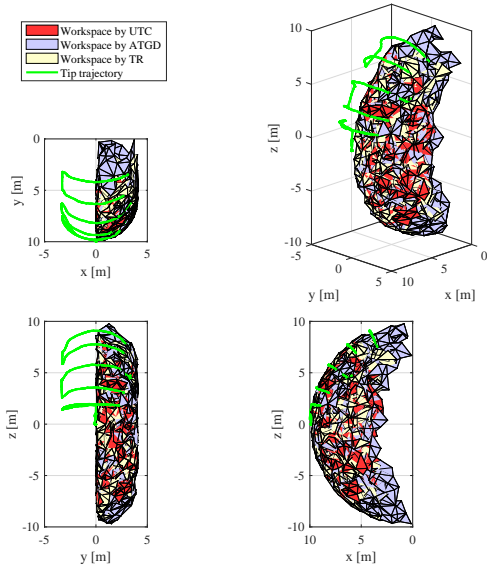


Fig. 9. Polygons of workspaces and tip trajectory. The tip trajectory in the experiment was set in the workspace obtained via ATGD.

The polygons shown in Fig. 9 are shaped like spherical shells. As shown in Fig. 6, 7, and 8, there are cross marks on the inside of each spherical shell, indicating the points at which the interior is beyond the range of joint movement. This implies that the workspace is narrow in the longitudinal direction of the manipulator. However, this longitudinally narrow workspace can be compensated for, because the manipulators used in nuclear facilities often possess a slider that moves the base in the longitudinal direction [7], [8].

The workspace of UTC is concentrated in the range of $|z| < 7$ m and $|y| < 4.5$ m. It can be seen that the workspace is limited to the vicinity in which the manipulator is extended fully. This is because the manipulator was mechanically designed to ensure that the tension in the straight orientation is low, and there existed a few choices for the joint angles in this orientation.

A clear drawback of ATGD is that its calculation time significantly exceeds than that required by UTC or TR. Although not a primary claim of this study, we attribute this increase in computation time to the use of iterative calculations in ATGD. Although TR also applies iterative calculations, it had the shortest calculation time. This is because TR only includes one optimization parameter and we used a high-speed CPU only for the computation of TR.

The volumes of the workspaces obtained via the UTC, TR, and ATGD approaches were determined to be 152, 180, and 222 m^3 , respectively. Thus, the proposed method expands the workspaces obtained by UTC and TR by 45% and 23%, respectively. The additional 23% represents the contribution of the yaw antagonistic tension to the expansion. By comparison, the workspace volume of the PAC robot manipulator [8], which comprises five links with a length of 1,250 mm, is estimated to be 149 m^3 . Although the workspace obtained

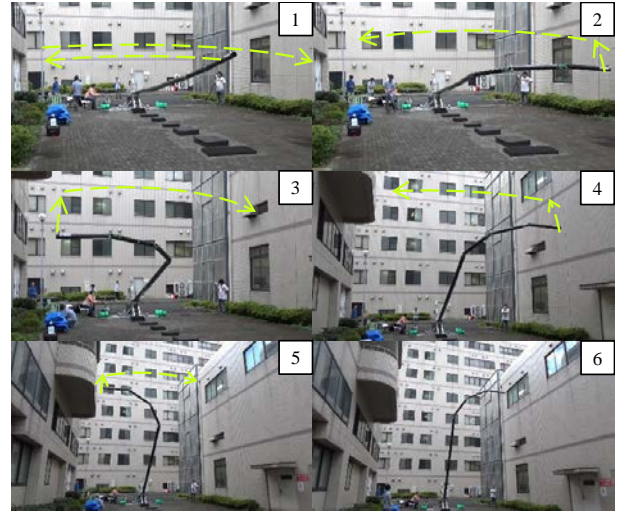


Fig. 10. Experiment carried out in workspace obtained via ATGD. The tip motion trajectory was successfully followed without breaking the tendons.

via UTC is only slightly larger than that of the PAC robot manipulator, the workspace obtained via the ATGD is 49% larger. This indicates that Super Dragon has a workspace that is comparable in size to that of other long-reach manipulators.

V. EXPERIMENT

We demonstrated the validity of the workspace obtained via the ATGD through experiments carried out using the actual manipulator. It is infeasible to use the arm and reach all positions contained in the workspace. Hence, we assessed one tip path to indicate that ATGD can expand the workspace. The path was not included in the workspace obtained via UTC but was included in that obtained via ATGD. It was expected that, if ATGD successfully enlarged the workspace, the tendons would not break.

The target tip path was set in advance. It was set to be similar to the exploration motion trajectory above horizontal ground. In Fig. 9, the target path is represented by the green line. The target trajectory of the joint angles was then obtained; specifically, the yaw joint angles θ_6 , θ_8 , and θ_{10} were swung to the left and right by $\pm 30^\circ$ and one pitch joint angle, θ_1 , was decreased by 15° in the direction of lifting of the manipulator. The pitch joint angles were kept constant at $\theta_2 = -6^\circ$ and $\theta_i = 0^\circ$ ($i = 3, 4, 5, 7, 9$). The angular velocity of joints was substantially static. During the experiment, the operator input the target trajectory to the manipulator and the tension of the tendons was controlled using ATGD. There were two different operating conditions from Section IV. The tension obtained through each iteration of the calculation was used as the initial value of the next iteration. The control was implemented using a Core i7-4910, 2.9 GHz, Intel. The maximum calculation time was 23 ms.

Fig. 10 shows the resulting motion of the manipulator, and Figure 11 shows the time courses of the joint angles. There were control deviations in the joint angles. Although the target angles θ_i , ($i = 3, 4, 5, 7, 9$) were always 0° , the pitch

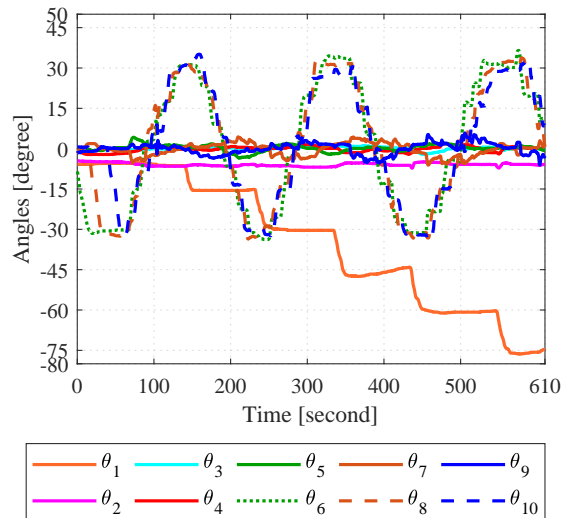


Fig. 11. Time courses of joint angles

joint angles changed over the course of the experiment. These variations were attributed to the inertia effect of the arm, wind, or friction. In addition, the positioning errors likely arose from the deformation of the structure, which can only be measured using an external sensor such as a laser tracker. These results indicate that the positioning accuracy of the system needs to be improved. However, the tendons did not fail and the measured tensions of the JCTs did not exceed 3kN. Overall, these experimental results indicate the validity of ATGD in terms of expanding the workspace.

VI. CONCLUSIONS

This study focused on the application of antagonistic tension on yaw joints in order to expand the workspace of a coupled tendon-driven articulated manipulator. To this end, a tension control method that combines the previously developed redundancy resolution method and gradient descent was proposed. The workspaces achieved by the proposed and conventional approaches were determined computationally, and the results were compared. The proposed method was capable of increasing the volume of the workspace by up to 45%. The results of an experiment with an actual robot suggested this expansion, while a comparison with previous research revealed that the Super Dragon possesses a large workspace.

In future research, we hope to reduce the calculation time of the proposed method and increase the accuracy of the workspace computation. It will also be necessary to model friction and develop a more global optimum method. We will conduct experiments involving additional paths and tests on positioning accuracy. Measuring the tension of tendons to demonstrate the effectiveness of the proposed method is also needed. Finally, we plan to determine whether the design of the pulley radii, structural matrix, and joint configuration are optimal.

ACKNOWLEDGMENT

This study is based on the results that were obtained from a project commissioned by the New Energy and Industrial Technology Development Organization (NEDO). This work was financially supported by the JAEA Nuclear Energy S&T and the Human Resource Development Project called concentrating wisdom (Grant Number JPJA19P 19210348).

REFERENCES

- [1] G. Endo, A. Horigome and A. Takata, "Super dragon: A 10-m-long-coupled tendon-driven articulated manipulator," *IEEE RA Letter*, vol. 4, no. 2, pp. 934941, Jan. 2019, doi: 10.1109/LRA.2019.2894855.
- [2] W. McMahan et al., "Field trials and testing of the OctArm continuum manipulator," *Proceedings 2006 IEEE International Conference on Robotics and Automation (ICRA)*, Orlando, FL, USA, 2006, pp. 23362341, doi: 10.1109/ROBOT.2006.1642051.
- [3] W. Xu, T. Liu and Y. Li, "Kinematics, dynamics, and control of a cable-driven hyper-redundant manipulator," in *IEEE/ASME Transactions on Mechatronics*, vol. 23, no. 4, pp. 16931704, Aug. 2018, doi: 10.1109/TMECH.2018.2842141.
- [4] J. Burgner-Kahrs, D. C. Rucker and H. Choset, "Continuum robots for medical applications: A survey," in *IEEE Transactions on Robotics*, vol. 31, no. 6, pp. 12611280, Dec. 2015, doi: 10.1109/TRO.2015.2489500.
- [5] Z. Wu, Q. Li, J. Zhao, J. Gao and K. Xu, "Design of a modular continuum-articulated laparoscopic robotic tool with decoupled kinematics," in *IEEE Robotics and Automation Letters*, vol. 4, no. 4, pp. 35453552, Oct. 2019, doi: 10.1109/LRA.2019.2927929.
- [6] T. Liu, Z. Mu, H. Wang, W. Xu and Y. Li, "A cable-driven redundant spatial manipulator with improved stiffness and load capacity," *2018 IEEE/RSJ International Conference on Intelligent Robots and Systems (IROS)*, Madrid, Spain, 2018, pp. 66286633, doi: 10.1109/IROS.2018.8593679.
- [7] "Fukushima Daiichi Nuclear Power Station The challenge of retrieving fuel debris Article No. 3: The frontier of technological development," 2020. [Online]. Available: https://www.enecho.meti.go.jp/en/category/special/article/detail_155.html
- [8] J. Chalfoun, C. Bidard, D. Keller, Y. Perrot and G. Piolain, "Design and flexible modeling of a long reach articulated carrier for inspection," *2007 IEEE/RSJ International Conference on Intelligent Robots and Systems*, San Diego, CA, USA, 2007, pp. 40134019, doi: 10.1109/IROS.2007.4399213.
- [9] S. Hirose and S. Ma, "Coupled tendon-driven multijoint manipulator," *Proceedings. 1991 IEEE International Conference on Robotics and Automation*, Sacramento, CA, USA, 1991, vol. 2, pp. 12681275, doi: 10.1109/ROBOT.1991.131786.
- [10] A. Horigome, H. Yamada, G. Endo, S. Sen, S. Hirose and E. F. Fukushima, "Development of a coupled tendon-driven 3D multi-joint manipulator," *2014 IEEE International Conference on Robotics and Automation (ICRA)*, Hong Kong, China, 2014, pp. 59155920, doi: 10.1109/ICRA.2014.6907730.
- [11] K. Yokoi, K. Tanie, N. Inamura, T. Kawai and K. Agou, "Design and control of a seven-degrees-of-freedom manipulator actuated by a coupled tendon-driven system," *Proceedings IROS '91: IEEE/RSJ International Workshop on Intelligent Robots and Systems*, Osaka, Japan, 1991, pp. 737742, doi: 10.1109/IROS.1991.174567.
- [12] H. Noborisaka and H. Kobayashi, "Design of a tendon-driven articulated finger-hand mechanism and its stiffness adjustability," *JSME International Journal Series C Mechanical Systems, Machine Elements and Manufacturing*, vol. 43, no. 3, pp. 638644, 2000, doi: <https://doi.org/10.1299/jsmec.43.638>.
- [13] S. Ma and M. Watanabe, "Minimum-time control of coupled tendon-driven manipulators," *Advanced Robotics*, vol. 15, no. 4, pp. 409427, Apr. 2012, doi: <https://doi.org/10.1163/156855301750398338>.
- [14] A. Horigome, G. Endo, K. Suzumori and H. Nabae, "Design of a weight-compensated and coupled tendon-driven articulated long-reach manipulator," *2016 IEEE/SICE International Symposium on System Integration (SII)*, Sapporo, Japan, 2016, pp. 598603, doi: 10.1109/SII.2016.7844064.
- [15] C. Gosselin and M. Grenier, "On the determination of the force distribution in over-constrained cable-driven parallel mechanisms," *Meccanica*, vol. 46, no. 1, pp. 315, 2011.
- [16] V. Salvucci, Y. Kimura, S. Oh and Y. Hori, "Force maximization of biarticularly actuated manipulators using infinity norm," in *IEEE/ASME Transactions on Mechatronics*, vol. 18, no. 3, pp. 10801089, June 2013, doi: 10.1109/TMECH.2012.2193670.

- [17] J. Lee and L. Tsai, "Torque resolver design for tendon-driven manipulators," *ASME. Journal of Mechanical Design*, vol. 115, no. 4, pp. 877883, Dec. 1993, doi: <https://doi.org/10.1115/1.2919282>.
- [18] A. Horigome, G. Endo, "Basic study for drive mechanism with synthetic fiber rope - investigation of strength reduction by bending and terminal fixation method," *Advanced Robotics*, vol. 30, no. 3, pp. 206217, Feb. 2016, doi: <https://doi.org/10.1080/01691864.2015.1102649>.
- [19] W. B. Lim, S. H. Yeo and G. Yang, "Optimization of tension distribution for cable-driven manipulators using tension-level index," in *IEEE/ASME Transactions on Mechatronics*, vol. 19, no. 2, pp. 676683, Apr. 2013, doi: [10.1109/TMECH.2013.2253789](https://doi.org/10.1109/TMECH.2013.2253789).
- [20] M. Gouttefarde, J. Lamaury, C. Reichert and T. Bruckmann, "A versatile tension distribution algorithm for n-DOF parallel robots driven by n+2 cables," in *IEEE Transactions on Robotics*, vol. 31, no. 6, pp. 1444-1457, Dec. 2015, doi: [10.1109/TRO.2015.2495005](https://doi.org/10.1109/TRO.2015.2495005).
- [21] J. Rastegar and B. Fardanesh, "Manipulation workspace analysis using the Monte Carlo method," *Mechanism and Machine Theory*, vol. 25, no. 2, pp. 233239, 1990, doi: [https://doi.org/10.1016/0094-114X\(90\)90124-3](https://doi.org/10.1016/0094-114X(90)90124-3).
- [22] J. Rastegar and D. Perel, "Generation of manipulator workspace boundary geometry using the Monte Carlo method and interactive computer graphics," *Journal of Mechanical Design*, vol. 112, no. 3, pp. 452454, Sep. 1990, doi: <https://doi.org/10.1115/1.2912630>.
- [23] Y. Nakamura, H. Hanafusa and T. Yoshikawa, "Task-priority based redundancy control of robot manipulators," *The International Journal of Robotics Research*, vol. 6, no. 2, pp. 315, Jun. 1987, doi: [10.1177/027836498700600201](https://doi.org/10.1177/027836498700600201).
- [24] J. Baillieul, "Avoiding obstacles and resolving kinematic redundancy," *Proceedings. 1986 IEEE International Conference on Robotics and Automation*, San Francisco, CA, USA, 1986, pp. 16981704, doi: [10.1109/ROBOT.1986.1087464](https://doi.org/10.1109/ROBOT.1986.1087464).
- [25] D. N. Nenchev, "Redundancy resolution through local optimization: A review," *Journal of Robotic Systems*, vol. 6, no. 6, pp. 769798, Dec. 1989, doi: <https://doi.org/10.1002/rob.4620060607>.
- [26] S. Ma, "Study of the optimal posture and tendon tension for coupled tendon-driven manipulator," *Transactions of the JSME*, vol. 63, no. 609, pp. 16651670, May 1997 (in Japanese).